Simulation of periodic counter-current chromatography purification of monoclonal antibodies with column degradation

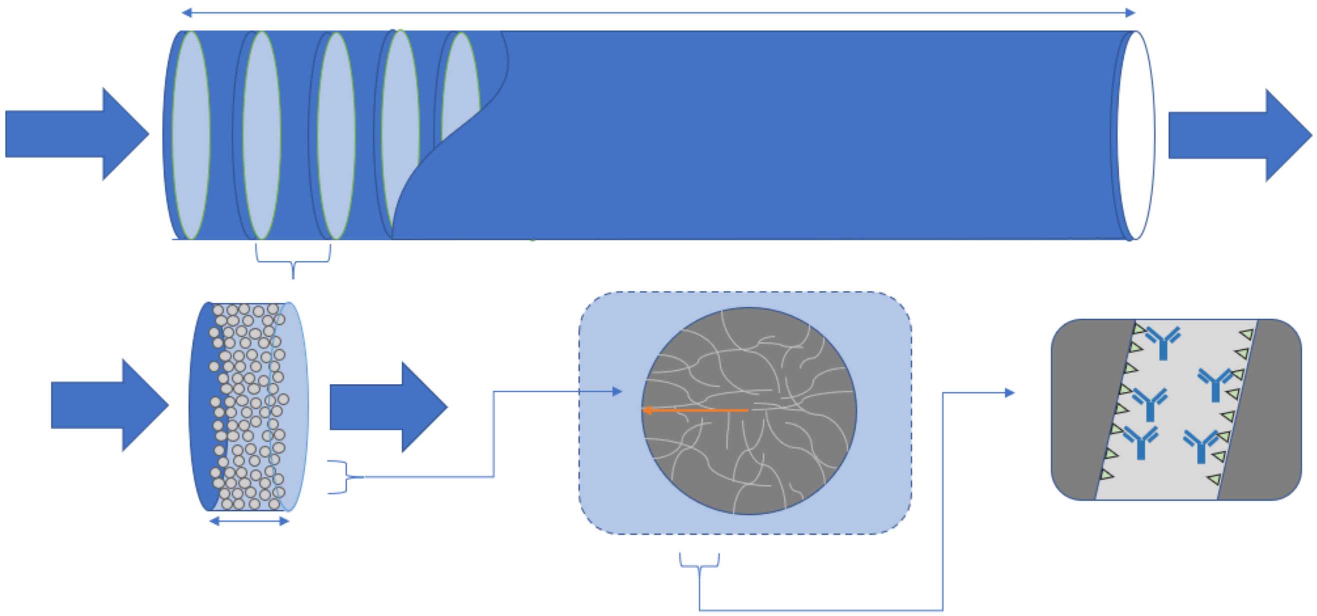

Erik Friberg

Department of Chemical engineering
Master Thesis 2022

LUND UNIVERSITY

Master thesis

Simulation of periodic counter-current chromatography purification of monoclonal antibodies with column degradation

By

Erik Friberg

Department of Chemical Engineering
Lund University

June 2022

Supervisor: **Associate senior lecturer Niklas Andersson**
Co-supervisor: **Postdoctoral fellow Joaquín Gomis Fons**
Examiner: **Professor Bernt Nilsson**

Front page picture: Domain discretization of an affinity chromatography column by Erik Friberg

Postal address	**Visiting address**	**Telephone**
Box 124	Kemicentrum	+46 46-222 82 85
SE-221 00 Lund, Sweden	Naturvetarvägen 14	+46 46-222 00 00
Web address	223 62 Lund, Sweden	
http://www.lth.se/chemeng/		

Printed in Sweden by Media-Tryck.
Lund 2022

Preface and acknowledgements

This thesis was written at the Department of Chemical Engineering at Lund University during the fall of 2021 and spring of 2022. The thesis was written over an unusual long period of time due to unforeseen personal hardship. The subject of the thesis is of interest for the department from a potential and economic perspective, in which chromatography columns might be able to be effectively utilized despite diminishing capacity.

I would like to thank my supervisor Niklas for all the help and encouragement I received when I felt stuck and needed someone to help me gather my thoughts and find new angles to tackle especially dicey problems. I’d also like to thank Joaquin for the days you spent in the lab showing me the PCC equipment and how the real process works. I really appreciated the meeting with my examiner Bernt as well, where we talked about the potential problems to tackle.

Lastly, I give a huge thanks to my loving girlfriend for all the moral support I was provided daily.

Summary

The purification process of monoclonal antibodies (mAbs) for therapeutic drugs is expensive, especially the chromatography step in which the mAbs are separated from other proteins and cells present in the feed. The antibodies are separated from the feed using affinity chromatography, where only the antibodies interact with active sites within the column, whereas the rest passes through the column without stopping. The antibodies leave the column when their chemical environment is changed, and the column is cleaned thoroughly with strong chemicals.

The chemicals are essential in the cleaning process to ensure that there is no contamination between cycles or that there are any antibodies left. The chemicals are however slightly damaging the column, and after many cycles of loading with mAbs, eluting the mAbs and then cleaning, the capacity of the column is reduced.

In this master thesis, periodic counter-current chromatography is modelled and simulated in python with columns that exhibit degradation. Two different controllers and a flow trajectory method is applied, to varying degrees, in different cases to investigate if they can counteract some of the problems that emerge due to the column degradation.

To evaluate the effectiveness of the controllers and the flow trajectory, the performance process variables productivity, yield, and resin utilization were used.

The best case used both controllers, the flow trajectory and had a productivity at 0.18 mg mAb per ml resin and minute, a minimum yield of 94.7% and a maximum resin utilization of 62.5 mg mAb per maximum amount adsorbed mAb at feed concentration.

Sammanfattning

Upreningsprocessen av monoklonala antikroppar (mAbs) är dyr, speciellt det kromatografisteg där antikropparna separeras från andra protein och celler i lösningen från tidigare steg i processen. Antikropparna separeras från lösningen med hjälp av affinitetskromatografi, där det endast är antikropparna som interagerar med innehåller i kolonnen och stannar kvar, medan resten passerar obehindrat. Antikropparna lämnar kolonnen när den kemiska omgivningen förändras och samlas upp, och kolonnen rengörs med starka kemikalier.

De starka rengöringskemikalierna är nödvändiga för att säkerställa att den inte sker någon kontaminering mellan cykler och att det inte sitter kvar några antikroppar. Kemikalierna skadar dock kolonnens innehåll något, och efter många cykler av antikroppupprening och rengöring, har kapaciteten hos kolonnen minskat.

I detta examensarbete har periodisk motströmskromatografi (PCC) modellerats och simulerats i programvaran Python tillsammans med kolonner som uppvisar degradering. Det används två olika regulatorer och flödestrajektoria, i varierande grad, i olika försök för att undersöka om de kan motarbeta de problem som skapas av degraderingen hos kolonnerna. Om kolonnerna, trots degradering, kan användas effektivt under längre tid till låg kapacitet återstår, är det möjligt att producera den upprenade antikroppen till ett lägre pris.

För att undersöka effektiviteten hos kontrollerna och av flödestrajektorian, kommer processprestandan utvärderas med hjälp av variablerna produktivitet, utbyte och utnyttjandegrad.

Det bästa fallet använde sig av båda kontrollerna, av flödestrajektorian och hade en produktivitet på 0.18 mg mAb per ml resin och minut, ett utbyte på 94.7% och en maximal utnyttjandegrad på 62.5 mg mAb per maximal mängd adsorberad mAb för flödeskoncentrationen.

Popular science summary

Antibodies are proteins that our bodies produce to protect us from infections. However, it is also possible to produce antibodies artificially in an industrial setting. These antibodies can then be used in a wide variety of research and clinical settings and their potential uses are evolving rapidly.

Artificially produced antibodies are typically produced by cells contained in large bioreactors under conditions where the cells are allowed to multiply. Cells containing antibodies are then continuously harvested. However, they typically need to be further purified after harvest. This can be done using a technique called affinity chromatography. In affinity chromatography, the harvested antibodies, including impurities such as other cell proteins, are fed to a column containing sites that capture the antibodies. After the impurities have been washed away, the antibodies get released from the column through a process of adjusting pH and salt concentrations. The column then needs to be chemically cleaned before it is ready to process more antibodies. Although necessary, the chemical cleaning process damages the column and decreases a column's ability to capture antibodies over time. It is therefore of interest to find ways in which the process can be run where the impact of the capacity reduction is minimal.

In this project, a so-called periodic counter-current chromatography (PCC) set-up was utilized to investigate ways to counteract the effects of column degradation. A mathematical model of a PCC system with three columns was created, and multiple simulations were performed in different cases to counteract the effects of column degradation.

Two different flowrate controllers and a flowrate trajectory were used in these cases. The flowrate controllers were each set to be fast, slow, or inactive, in different configurations. Each configuration was run twice. Once with flowrate trajectories and once without. The simulations were compared to each other using the processes performance variables productivity, yield and column utilization.

The best case had a productivity of 0.18 mg mAb per ml resin and minute, a yield of 94.7% and resin utilization of 62.5 mg mAb per maximum amount adsorbed mAb at feed concentration. This case was chosen for its high productivity (in the range 0.11 – 0.20), acceptable yield (ranges from 88 – 100%), and good resin utilization (in range 40.2 – 77.5).

Populärvetenskaplig sammanfattning

Antikroppar är proteiner som produceras av våra kroppar för att skydda oss från infektioner. Det är däremot möjligt att producera dessa antikroppar artificiellt. Dessa antikroppar kan sedan användas i en mängd olika forsknings- och kliniska miljöer och deras potentiella användningsområden utvecklas snabbt.

Artificiellt producerade antikroppar produceras vanligtvis av celler i stora bioreaktorer under förhållanden där cellerna tillåts föröka sig. Celler som innehåller antikroppar skördas sedan kontinuerligt. Men de behöver vanligtvis renas ytterligare efter skörd. Detta kan göras med en teknik som kallas affinitetskromatografi. Vid användandet av affinitetskromatografi matas de skördade antikropparna, inklusive föroreningar såsom andra cellproteiner, till en kolonn som innehåller platser som fångar antikropparna. Orenheterna spolas bort och efter justerat pH och salt koncentration släpper antikropparna från de aktiva platserna och fångas upp vid hög koncentration. Kolonnen spolas och renas kemiskt innan den är redo att rena upp mer antikroppar. Den kemiska rengöringen är viktigt men den skadar kolonnen vilket med upprepade cykler leder till en minskad kapacitet hos kolonnen. Det är därför av intresse att hitta sätt som processen kan köras på där påverkan av kapacitetsminskningen blir minimal.

I detta examensarbete användes en set-up kallad periodisk motströmskromatografi (PCC) för att undersöka hur effekterna av kolonndegraderingen kunde motverkas. En matematisk modell av ett PCC-system med tre kolonner skapades och flertalet simulationer utfördes för olika fall där kolonndegraderingens effekter motverkades.

I dessa olika fall användes det två flödesregulatorer och en flödestrajektoria. Flödesregulatorerna var snabba, långsamma eller inaktiva, i olika konfigurationer. Varje konfiguration utfördes två gånger. En gång med flödestrajektoria och en gång utan. Simulationernas processprestanda jämfördes mot varandra med hjälp av variablerna produktivitet, utbyte och utnyttjandegrad.

Det bästa fallet hade en produktivitet på 0.18 mg mAb per ml resin och minut, ett utbyte på 94,7% och en maximal utnyttjandegrad på 62.5 mg mAb per maximal mängd adsorberad mAb för flödeskoncentrationen. Detta fall valdes på grund av sin höga produktivitet (bland resultat inom spannet 0.11 – 0.20), sitt acceptabla utbyte (inom spannet 88 – 100%) och sin goda utnyttjandegrad (i spannet 40.2 – 77.5).

Table of contents

1. Introduction

1.1 Overview

The Covid-19 pandemic gave rise to enormous efforts being put towards finding a vaccine and therapeutic medicines to use on patients with severe symptoms (Hwang, Lu et al. 2022). Many of the new therapeutic medicines were based on monoclonal antibodies (mAbs), which are large proteins that the body naturally produces to fend of infections and viruses (Lu, Hwang et al. 2020). Antibody production can be stimulated in the body by vaccines, but it takes time for the body to start producing its own. If the virus in question is known, manufactured, highly specific and target seeking antibodies can be used to stop the virus.

This master thesis will focus on the manufacturing process of said antibodies; the purification using Protein A columns with periodic counter-current chromatography (PCC) and how the degradation of the resin affects the process and if there is a way to control the process in order to counteract the negative consequences that the degradation has on the process.

1.2 Aim

The aim of this master thesis is to investigate the process performance variables, yield, productivity, and resin utilization, of the PCC process of purifying antibodies when applying column degradation to the simulation. Different cases will be evaluated by applying a flowrate controller, a volume regulation controller, and flow trajectories to investigate how the column degradation affects the system, and if the controllers are able to maintain the process at reasonable performance.

2. Background

The first part of the background explains the many usages of monoclonal antibodies within the medical field. The next part is about chromatography, then affinity chromatography and periodic counter-current chromatography, and lastly process economy and column degradation.

2.1 Monoclonal antibodies (mAbs)

The technique to develop monoclonal antibodies (mAbs) was invented by Köhler and Milstein in 1975, yielding them a Nobel Prize in 1984. mAbs are large protein molecules in a Y-shaped structure that is formed by two different proteins held together by disulfide bonds. They are used therapeutically in oncology and to treat immunological/infectious diseases, but its use is expanding into other disease areas as well (Castelli, McGonigle et al. 2019).

In 2018, the global therapeutic mAbs market was roughly valued at US$115 billion and is expected to exceed revenues of US$300 billion by 2025 (Lu, Hwang et al. 2020).

For treatment of autoimmune diseases, mAbs are most often used to block signaling molecules from inducing vasodilation and inflammation. There are other mechanisms as well, but what they all have in common, within this field, is that they work to suppress excessive responses by the immune system (Castelli, McGonigle et al. 2019).

In oncology mAbs are used to target tumor antigens and overly expressed receptors on tumor cells, to weaken or kill said tumor cells. For example, growth factor receptors can be blocked in breast cancer tumors. This decreases the tumor growth rate, increases the tumor sensitivity towards chemotherapy and initiates programmed cell death. Another example is to target antigens on the tumor surface to stimulate inflammation, which causes phagocytosis (macrophages envelopes afflicted cells, breaks them down into components and presents them to the immune system) or directly kills the targeted cells (Castelli, McGonigle et al. 2019).

Monoclonal antibodies are also used to treat hepatitis A and B, and multidrug-resistant HIV-1 infections among other infectious diseases. Development of mAbs for other diseases such as Ebola virus disease, hepatitis C and herpes simplex virus, is ongoing (Castelli, McGonigle et al. 2019).

Given mAbs ability to treat infectious diseases and virus infections, remarkable efforts has been made in biomedical laboratories around the world the last two years to develop therapeutics, prophylactics and diagnostic tools to tackle the COVID-19 pandemic (Hwang, Lu et al. 2022).

In conclusion, the use of mAbs is currently indicated in a wide variety of clinical situations. Furthermore, ongoing medical research is constantly expanding the implications for mAbs usage to save lives.

2.2 Chromatography

Chromatography is a separation method used to purify biological or chemical compounds from a liquid mobile phase, using a stationary phase with which compounds interact to varying degrees. Compounds that interact more with the stationary phase stays longer inside the column and those that interact less, exit the column faster, creating the desired separation (Hage 2012). The difference in equilibrium constants of the components in the mobile and the stationary phase, determines how well the components in the mobile phase separate from each other (Diefenbach-Streiber, Enzelberger et al. 2010).

The mobile phase can be either a gas, as in gas chromatography (GC) where the stationary phase is a liquid or a solid, or a liquid, as in liquid chromatography (LC) where the stationary phase is a solid. The two phases, gas – liquid, gas – solid or liquid – solid, are in relative motion to each other, usually in a tubular column (Strube, Zobel-Roos et al. 2019).

The system discussed in this thesis is a liquid chromatography system. Affinity chromatography is a special liquid chromatography technique and will be further explained in the next section.

2.3 Affinity chromatography

In affinity chromatography, the structural elements on the target molecule and the immobilized ligand have a highly selective interaction. The high selectivity is due to the utilization of functional biological interactions, such as the very selective antibody-antigen-, and enzyme-inhibitor-interactions, to name a few. The affinity chromatography technique typically has high binding capacity combined with outstanding selectivity, this results in short processing times and good robustness of the process (Danielsson 2018).

Affinity chromatography is used at all scales within the biochemical field, from laboratory settings to the industrial scale, to analyze, capture, and purify specific protein-based biomolecules. The method is especially useful in the downstream processing of the bioprocess industry, as it is the most cost-effective way to produce therapeutic monoclonal antibodies (mAbs) (Hage 2012, Jagschies 2018).

Clever scheduling, process control and precise machine switches has enabled the method to function continuously. One of these techniques is called periodic counter-current chromatography (PCC – for short). More about this topic in section.

2.4 Design for the capture of mAbs

These are the different operations performed on the column to separate the mAbs form impurities, such as host cell proteins (HCP), and prepare the column for another cycle.

1. Load

   The feed containing the mAbs and HCP flows through the column under pressure from a pump. The flow rate and load time is determined by the volume of the column, the concentration of the feed, the dynamic binding capacity for the active sites within the column matrix. HCP will be visible in the outflow after roughly one column volume has been fed, as they pass through the column without interaction. The mAb concentration in the outflow is zero until the column is no longer able to bind the mAbs to the active sites at a sufficient rate. As the binding rate decreases because of the diminishing amount of available active sites left, the mAb concentration in the outflow increases, see figure 2.1 for a visualization of the breakthrough curve for the HCP and the mAbs. The load operation will stop either after a set amount of time or when the mAb concentration reaches a certain UV-signal value in the outlet flow.

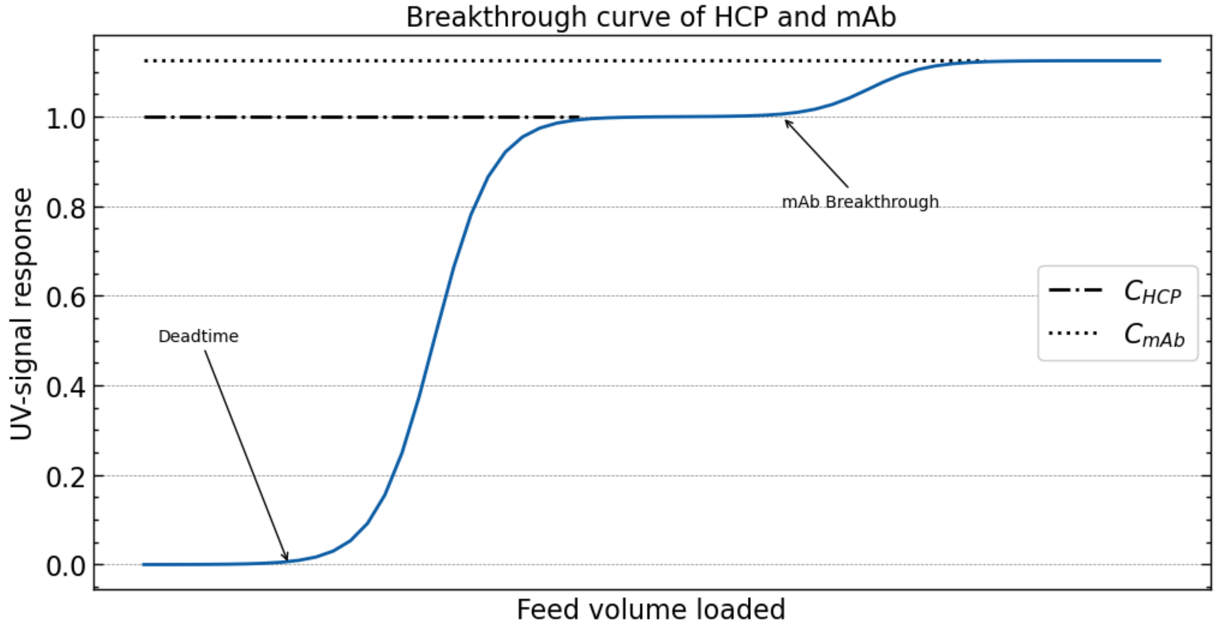

Figure 2.1. Breakthrough curve. The deadtime of the system is when one column volume of feed has passed through the column and HCP starts eluting. The mAb breakthrough is visible when the second curve starts eluting.

2. Wash

The wash removes impurities from the column, leaving the adsorbed mAbs behind.

3. Elution

The mAbs will leave the active sites by changing the pH and/or salt concentration in its immediate surroundings. All sites will be vacated with the pH and salt change, leading to a highly concentrated pulse of mAbs that is collected at the column outlet. The mAbs is now substantially more concentrated than before the separation, and the collected liquid contains only miniscule amounts of impurities if compared to the feed.

4. Clean-in-place (CIP)

The column might still contain some mAbs and contaminants which may cause problems if left to accumulate. Fouling by blockage or microbial growth, could potentially ruin the column. Cleaning-in-place (CIP) is best done by using strong chemicals, such as sodium hydroxide. If the concentration of NaOH is too low, the cleaning will be insufficient, but if too high, the carrier material hosting the active sites may take structural damage and degrade. Some materials are more resilient to chemical degradation and can thus withstand harsher cleaning procedures.

5. Equilibration

The active sites need to be equilibrated to bind mAbs once again.

The time it takes for the system to go through each step, one through five, is called the cycle time.

2.5 Periodic counter-current chromatography (PCC)

Periodic counter-current chromatography is a continuous separation process as it can process a continuous feed with clever scheduling of batch operations. The switch times are either predefined from experiments or by using UV-detectors, before and after the column being loaded (Jagschies 2018). The host cell proteins (HCP) are not captured in the column and exits the column first and creates a steady UV-signal profile. When the active sites in the column starts to become saturated with mAbs and mass transfer resistance limits the adsorption rate, the mAbs escape the column through the outlet and the UV-signal increases slightly but steadily to a new higher output level, see figure 2.1.

The Protein A resins used in the columns for the purification of mAbs can differ in active site density and the size of the particles in which the active sites are located. The static binding capacity (SBC) of the resin is the maximum amount of mAbs the resin is able to hold, but when used in PCC the resin capacity is often not used to the fullest capacity as the load time would be very long, with a slow flowrate, or a lot of mAbs would flowthrough the column and possibly be lost. Another parameter called the dynamic binding capacity (DBC) is often used to characterize different resins. It’s an experimental measure of how much mAbs that has adsorbed to the resin when the breakthrough percentage reaches 10%. It’s measured in mg mAbs per ml resin. However, the DBC is dependent on the flowrate and the feed concentration. The DBC is thus better for describing the resin binding capacity under realistic run conditions (Ebersbach and Geisse 2012).

In PCC the mAbs that escape the first column is caught by a second column that is coupled in series with the first, which prevents losses of mAbs (see figure 2.2), in contrast to batch affinity chromatography where mAbs are either lost to waste or the capacity of the column is unutilized to a much larger extent to prevent losses. This coupling of columns in series allows the columns capacity to be utilized to greater extent and prevents the loss of mAbs at the same time (Jagschies 2018).

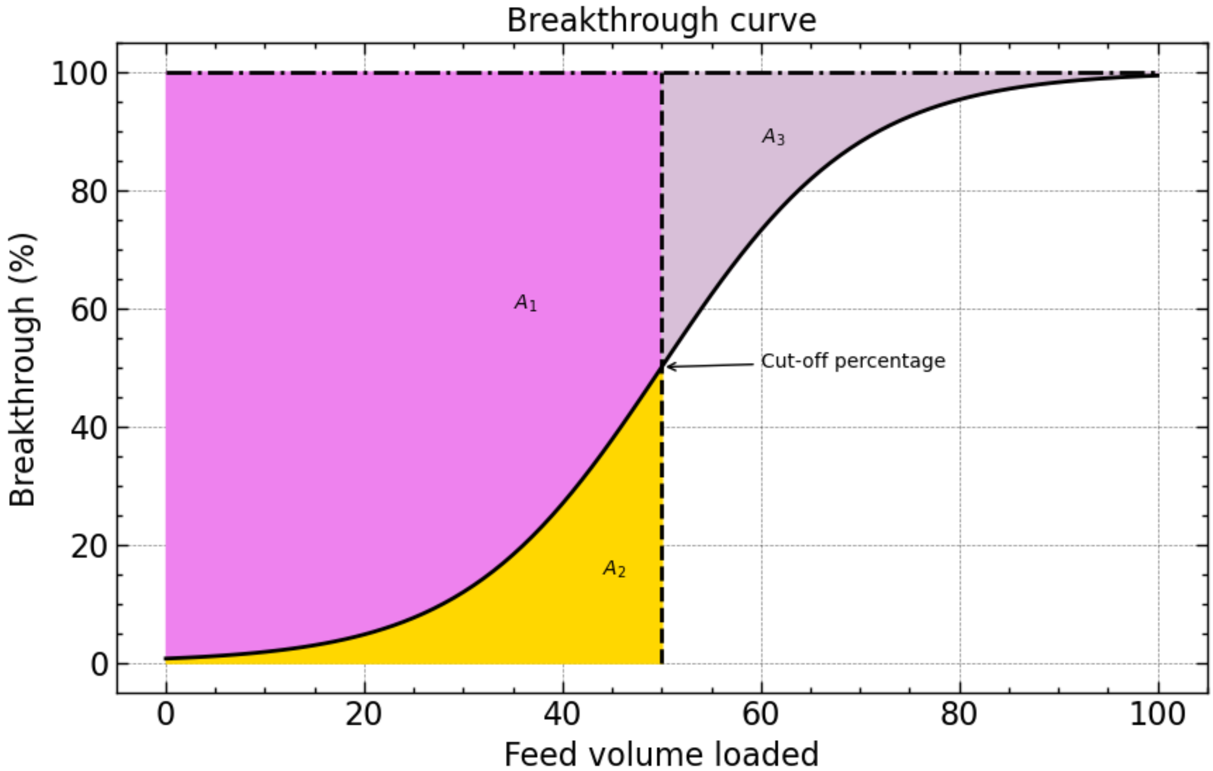

Figure 2.2. Breakthrough curve. Relationship between the feed volume loaded and the captured mAb in the first and second column. The area A_1 is the mAb captured by the first column, the area A_2 is the mAb captured by the second column. A_3 is unused capacity in the first column. The cut-off percentage is the breakthrough value at which the phase ends. (Inspired by Figure 3 in (Lofgren, Gomis-Fons et al. 2021))

The same idea is applied to the wash process as there are still mAbs in the mobile phase when the loading phase for a saturated column is ended. The cycle arrangement for the PCC process is described in figure 2.3.

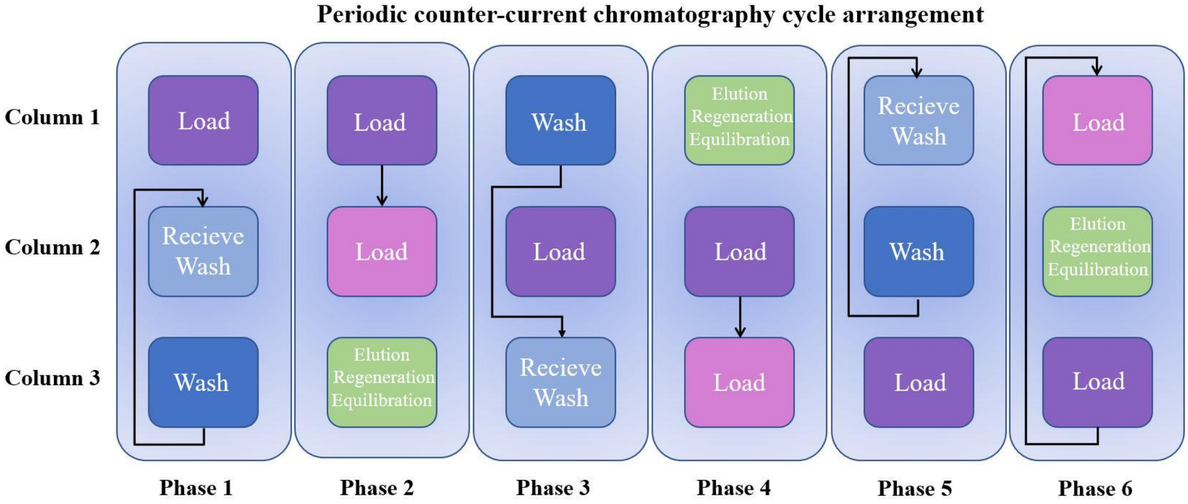

Figure 2.3. The periodic counter-current chromatography cycle arrangement consists of six different phases. Each row represents a chromatography column, and, in each phase, the column may be interacting with another column or performing an operation on its own. When all phases have been performed, the system starts over on phase one again, as the new cycle begins.

2.6 Process economy and column degradation

Manufacturing mAbs is costly, largely due to the downstream costs, as there are strict purity requirements for the final product. The chromatography process step is estimated to stand for up to 60% of the total downstream costs. The price of the protein A resin is a large contributor to the large percentage, which is why it's imperative to use the resin in a cost-effective manner (Danielsson 2018).

The column degradation determines how many cycles the columns can be used before they need to be replaced. Protein A resins are often used between 100 and 200 cycles (Danielsson 2018). The degradation of the resin takes place during the cleaning cycle where the column is washed and disinfected with strong alkaline solutions. The dynamic binding capacity is decreased, and the breakthrough curve appears earlier and earlier if the flow rate is constant.

3. Methods for modelling and simulation

To investigate how the degrading column capacities affect the PCC process, the capture step was modelled using the modified general rate model (Gomis-Fons, Andersson et al. 2020).

The simulation was performed in Python 3.8 and the set-up is explained later within this section.

3.1 Process model

The binding mechanism for this model is assumed to be heterogeneous with both fast and slow binding sites. Eq. 1 describes the concentration in the mobile phase, while Eq. 2 describes the concentration within the particles. The boundary conditions for the concentration equations are presented in Eqs. 1.1, 1.2, 2.1 and 2.2. The binding kinetics is described by Eq. 3.

$$\frac{\partial c}{\partial t} = D_{ax}\frac{\partial^2 c}{\partial z^2} - \frac{v}{\varepsilon_c}\frac{\partial c}{\partial z} - \frac{1-\varepsilon_c}{\varepsilon_c}\frac{3}{r_p}k_f\left(c - c_p\big|_{r=r_p}\right) \qquad (1)$$

Where c is the concentration of monoclonal antibodies (mAb) in the mobile phase, D_{ax} is the axial dispersion coefficient, v is the superficial fluid velocity, ε_c is the column void, k_f is the mass transfer coefficient in the particle layer, and c_p is the mAb concentration in the outermost layer of the particle.

$$\frac{\partial c}{\partial z} = \frac{v}{\varepsilon_c D_{ax}}\left(c - c_f\right) \qquad at\ z = 0 \qquad (1.1)$$

$$\frac{\partial c}{\partial z} = 0 \qquad at\ z = L \qquad (1.2)$$

Eq. 1.1 is the boundary condition at the beginning of the chromatography column, where c_f is the inlet mAb concentration. Eq. 1.2 is the boundary condition at the column outlet.

$$\frac{\partial c_p}{\partial t} = D_{eff}\frac{1}{r^2}\frac{\partial}{\partial r}\left(r^2\frac{\partial c_p}{\partial r}\right) - \frac{1}{\varepsilon_p}\frac{\partial(q_1+q_2)}{\partial t} \qquad (2)$$

Where c_p is the mAb concentration within the particle, D_{eff} is the effective pore diffusivity, r is the particle radius, ε_p is the particle porosity, q_1 and q_2 is the adsorbed mAb concentration onto the fast respectively slow adsorption sites.

$$\frac{\partial c_p}{\partial r} = 0 \qquad at\ r = 0 \qquad (2.1)$$

$$\frac{\partial c_p}{\partial r} = \frac{k_f}{D_{eff}}\left(c - c_p\right) \qquad at\ r = r_p \qquad (2.2)$$

The boundary conditions for the center of the particle is described by Eq. 2.1., and the boundary condition at the surface of the particle is described by Eq. 2.2.

$$\frac{\partial q_i}{\partial t} = k_i[\left(q_{max,i} - q_i\right)c_p - \frac{q_i}{K}] \qquad (3)$$

Where k_i is the adsorption rate constant, q_{max} is the maximum adsorption capacity, K is the Langmuir equilibrium constant, and i can be 1 for fast kinetics and 2 for slow kinetics.

3.2 Degradation model

The degradation of the resin static binding capacity, as seen in table 1, was investigated by Wetterhall et al. for the MabSelect PrismA affinity chromatography column for NaOH concentrations between 0.1 – 2.0M and clean-in-place incubation time up to 72 hours (Wetterhall, Ander et al. 2021). The MabSelect PrismA column manufacturer, Cytiva, disclosed in a technical report that the dynamic binding capacity of the ÄKTA Pure PrismaA resin (at 10% breakthrough) decreased by 10% after 150 cycles of CIP with 15 minutes of contact time of 1M NaOH per cycle (Cytiva 2020).

Table 3.1 Static binding capacity (SBC) of the MabSelect PrismA affinity chromatography column after being in contact with 1M NaOH solution for different lengths of time.

Time [h]	0	1	4	8	16	24	48	72
SBC [%]	100.00	98.89	100.59	101.76	97.56	96.45	89.05	75.50

Using the same residence time at 15 min and concentrations of NaOH for the CIP as in the Cytiva product report, the degradation curve can be found by curve fitting the data from Wetterhall et al. to Eq. 4.

$$Y = a * x^2 + b \quad (4)$$

3.3 Volumetric flow control

Iterative learning control is often used to control machines performing repetitive tasks, in this case a PCC machine. The controller observes the difference between the system outcome and the desired outcome, and using a feedback controller and the learning law makes small changes between iterations to decrease the error (Longman 2010)

Two controllers were used to control the flowrate.

Both controllers are inspired by an article previously published by Löfgren and Gomis-Fons (Lofgren, Gomis-Fons et al. 2021). The controllers are iterative learning controllers, taking inputs from the previous iteration (u_{k-1} and y_{k-1}) to calculate the change in variables for the next iteration (u_k) to minimize the error between a reference value (y_{ref}) and the value produced by the simulation (y_k).

The control signal for iteration k (u_k), where k is an integer larger than zero, is calculated using the difference between the reference signal (y_{ref}) and the output signal from the previous iteration (y_{k-1}), times the controller gain (K), plus the control signal from the previous iteration (u_{k-1}), see equation 5.

$$u_k = u_{k-1} + K(y_{ref} - y_{k-1}) \quad (5)$$

The output signal (y_k) can be calculated by multiplying the control signal (u_k) with a transfer function (G), which is a linear approximation of the process that takes no account of any possible measurement errors or system uncertainties, see equation 6. In the system where these controllers are applied, we assume that there are no measurement errors nor system uncertainties.

$$y_k = Gu_k \tag{6}$$

Convergence is when the error between the reference value and the output signal tend to zero, and this is a design criterion that must be fulfilled for the selection of the controller gain (K), see equation (7).

$$\|1 - GK\| = a < 1 \tag{7}$$

Equation 7 can be rewritten to define K as a function of the parameter a, which is larger than zero and smaller than one, times the inverse transfer function (G^{-1}), see equation 8.

$$K = (1 - a)G^{-1},\ 0 \leq a \leq 1 \tag{8}$$

The addition of the parameter a adds the ability to let the controller act on the system with variable aggression. An a-value close to 0 will allow the changes between iterations to be much larger than an a-value close to 1. The drawback on letting the a-value be low is that it increases the risk of divergence and oscillations.

By combining equation 8, 6 and 5, the control law for the system can be rewritten, where the control signal for the next iteration is dependent on the reference value (y_{ref}), the previous iteration output (y_{k-1}) and input (u_{k-1}), and the parameter a, see equation 9.

$$u_k = u_{k-1}(a + (1 - a)\frac{y_{ref}}{y_{k-1}}) \tag{9}$$

The controllers used in the simulation are based on equation 9. The first controller, equation 10, will be called the flowrate controller, where u_k is the flowrate F in ml/min, $y_{ref,k}$ is the amount of mAb captured by one column in one cycle.

$$u_k = u_{k-1}\left(a_1 + (1 - a_1)\frac{y_{ref,k}}{y_{k-1}}\right),\ 0.3 \leq u_k \leq 1.5 \tag{10}$$

The other controller, equation 11, is the volume regulation controller, where $y_{ref,k}$ is an amount of captured mAb, $y_{ref,vol}$ is the reference volume set during the set-up of the simulation and $y_{vol,k-1}$ is the feed volume processed in the previous PCC cycle.

$$y_{ref,k} = y_{ref,k-1}(a_2 + (1 - a_2)\frac{y_{ref,vol}}{y_{vol,k-1}}) \tag{11}$$

The controllers are only active in phase 2, 4 and 6, when the columns are coupled in series. In phase 1,3 and 5, the column load phase is constant, with a feed flow of 0.8 ml per minute for 6 minutes. This equals a load of 4.6 ml per column.

When both controllers are active, the volume regulation controller changes the y_{ref} of the flowrate controller and to prevent that the simulation diverges in a way that causes Python to crash, the flowrate controller signal (u_k) is limited to the interval 0.3 to 1.5.

3.4 Flowrate trajectories

A flowrate trajectory is several different flowrates that integrated over time will produce the same volume as a constant flowrate integrated over the same time. The shape of the flowrate trajectory applied to the PCC process that has shown the best productivity improvement, is a stepwise decreasing flowrate (Gomis-Fons, Yamanee-Nolin et al. 2021).

The flowrate trajectory used will follow the percentages and relative cut-times as presented in table 3.2. The load time will be reduced to 90% of the original load time, as this produced an improvement in productivity. The load volume will remain the same.

Table 3.2. The flowrate is multiplied with the percentage presented below, when the time is within the corresponding time interval. The values were extracted from figure 3.A Case IIb in (Gomis-Fons, Yamanee-Nolin et al. 2021).

Flowrate (%)	**176.44**	**131.25**	**89.90**	**84.62**	**74.04**
Time	0 – 0.2	0.2 – 0.4	0.4 – 0.6	0.6 – 0.8	0.8 – 1.0

In the beginning of the load phase, the flowrate is high, and the adsorption rate is high. As the loading time progresses, the flowrate decreases at a pace that is roughly matched by the columns ability to bind mAbs to the particles. The decreased flowrate at the end of the loading phase lets the concentration of mAbs be as high as possible for as long as possible within the column. The flow trajectory enables the column to adsorb more mAbs in shorter time.

3.5 Productivity, yield, and resin utilization

To measure the process performance, three variables will be defined.

Productivity of the PCC process is defined as the amount mAbs captured divided by the amount of resin used and the of the time it took to capture the mAbs, see equation 10. Productivity is expressed in mg mAbs adsorbed per ml resin and minute.

$$P = \frac{m_{ads}}{t_{cycle}V(1-\varepsilon_c)} \qquad (12$$

The variable m_{ads} is defined as the mAbs captured by all columns during the cycle. This includes the solitary loading and wash of the columns in phase 1, 3 and 5, as well as the flowthrough to the second column in the series in phase 2, 4 and 6. V is the combined volume of the three columns and ε_c is the column void.

The yield of the process is defined as the amount of mAbs captured over the amount mAbs fed to the process, see equation 11. Yield is expressed as a percentage.

$$Y = \frac{m_{ads}}{m_{in}} \qquad (13)$$

The variable m_{ads} is the same as in the previous expression. m_{in} is the sum of all individual flowrates, times the feed concentration for the cycle.

The resin utilization is defined as the amount of mAbs captured over the maximum amount of mAbs that can be captured using the feed concentration, see equation 12. The resin utilization is expressed as the amount of mAbs captured over the maximum amount of mAbs captured for the concentration of mAbs in the feed and available active sites.

$$U = \frac{m_{ads}}{D_{d,n}(q_{max,1}+q_{max,2})K*c_f(\frac{1}{1+K*c_f})} \quad (14)$$

The variable m_{ads} is the same as in the previous two expressions. $D_{d,n}$ is the degree of degradation at cycle n, $q_{max,1}$ and $q_{max,2}$ is the maximum adsorption capacity for fast and slow adsorption sites, K is the Langmuir equilibrium constant and c_f is the mAbs concentration in the feed.

The different cases can be compared to each other using these process variables and the parameters set for the controllers can be evaluated to understand how and if they improve the performance of the process with the column degradation at work.

3.6 Simulation set-up

The simulation was performed in Python 3.8 with the additional packages numpy, matplotlib.pyplot, solve_ivp from scipy.intregrate, FVMtools, time, and lastly curve_fit from scipy.optimize.

The columns were simulated using two different models. The first model is for one column and is used in the PCC cycle for phase 1, 3, and 5. The second model contained two columns coupled in series and is used in the PCC cycle for phase 2, 4 and 6, where the output concentrations from the first column is the input for the second.

The column length is discretized into 10 equal parts, and particle radius in each column part is further discretized into 30 equal parts. The discretization is set up in this way, so that values from the article by Gomis-Fons, Andersson, and Nilsson (Gomis-Fons et al., 2020) could be used, as their model used the same discretization when it was calibrated from experimental values.

The simulations of both models are calculated using solve_ivp with the BDF method, jacobian matrices, atol and rtol of 1e-7, a constant time span of 6 minutes, and 960 initial values for the first model and 1920 for the second model, defining the concentration of mAb and HCP throughout the columns and the resin particles.

To increase the speed of the solver (solve_ivp), Jacobian matrices were used for the initial values to each model.

The simulation starts with a feed flow rate of 0.8 ml/min and the cut-off percentage is 6% for first 3 cycles, as part of the start-up for the process. The cut-off percentage is implemented using an event function in solve_ivp. After the three start-up cycles, the controllers are engaged, u_0, $y_{ref,vol}$ and $y_{ref,0}$ is set and the simulation is then run for six cycles near 100% resin capacity to stabilize. The simulation then jumps ahead to 5 cycles before the resin capacity in the column reaches 95%. It performs 6 cycles (so that the resin capacity is 95% for the last one), before taking another jump. This repeats until the last series of simulations are performed with the final resin capacity at 75%.

The column capacities and the cycle numbers are connected via the degradation model.

3.7 Cases

To see the impact of the controllers on the process performance variables and how they compare to each other at different stages of degradation, 12 cases are presented below.

In case 1 and 2, the parameter a-values 0.80 and 0.30 are used. For case 1, the a-values associated with the flowrate controller is 0.80 and the a-values for the volume regulator is 0.30. For case 2, the a-values associated with the flowrate controller is 0.30 and the a-values for the volume regulator is 0.80.

In case 3 and 4, the parameter a-values 0.30 and 1.00 are used. For case 3, the a-values associated with the flowrate controller is 0.30 and the a-values for the volume regulator is 1.00. For case 4, the a-values associated with the flowrate controller is 1.00 and the a-values for the volume regulator is 0.30.

Each case 1 through 4 are simulated twice. One time using the flow trajectories and one time without. The flowrate trajectory simulation of each case is associated with the letter A, following the number of the case. If the simulation was performed without the flowrate trajectories, the letter following the number is B.

The first eight cases are presented in table 3.3.

Table 3.3. Description of case variables for Case 1A through Case 4B.

Case	**a_1 (Flowrate controller)**	**a_2 (Volume regulator)**	**Flowrate trajectories**
1A	0.80	0.30	ON
1B	0.80	0.30	OFF
2A	0.30	0.80	ON
2B	0.30	0.80	OFF
3A	0.30	1.00	ON
3B	0.30	1.00	OFF
4A	1.00	0.30	ON
4B	1.00	0.30	OFF

The remaining four cases are Case X1, X2, X3, and X4. These cases are focused on the divergence of the system and a way to deal with it.

In Case X1, the a_1-value is 0.30 and the a_2-value is 0.65. In Case X2, the a_1-value is 0.30 and the a_2-value is 0.60.

In Case X3 and X4, the columns are given individual a_1 values. The speed of the controllers now varies from column to column. The a_1-value for the first column is annotated $a_{1,1}$, for the second column $a_{1,2}$, and lastly the third column $a_{1,3}$.

The variables for Case X3 are: $a_{1,1}$ is 0.30, $a_{1,2}$ is 0.35, $a_{1,3}$ is 0.40, and a_2 is 0.60. The variables for Case X4 are: $a_{1,1}$ is 0.30, $a_{1,2}$ is 0.35, $a_{1,3}$ is 0.40, and a_2 is 0.50.

Flowrate trajectories are active for all simulations X1 through X4, and a summary of the cases can be seen in table 3.4.

Table 3.4. Description of case variables for Case X1 through Case X4.

Case	**a_1 (Flowrate controller)**			**a_2 (Volume regulator)**	**Flowrate trajectories**
X1	0.30			0.65	ON
X2	0.30			0.60	ON
	$a_{1,1}$	**$a_{1,2}$**	**$a_{1,3}$**		
X3	0.30	0.35	0.40	0.60	ON
X4	0.30	0.35	0.40	0.50	ON

Variables that were kept constant between cases are presented in appendix A. The control parameter for the flowrate controller had lower and upper limits at 0.3 and 1.5, as the simulation accuracy is drastically reduced outside of these limits.

4. Results

The starting condition for each case is identical; a start-up phase followed by three PCC cycles with a cut-off at six percent, as seen in figure 4.1. The set-up produced the reference values for the flowrate and the volume regulation controller, with $Y_{ref,k}$ being 48.09 mg captured mAbs and $Y_{ref,vol}$ being 305.75 ml of processed feed during one PCC cycle. The load time for the loading of column in series was constant at 109 minutes and 15 seconds for the simulation when the flow trajectories were active, and 121 minutes and 24 seconds for when the flow trajectories were turned off.

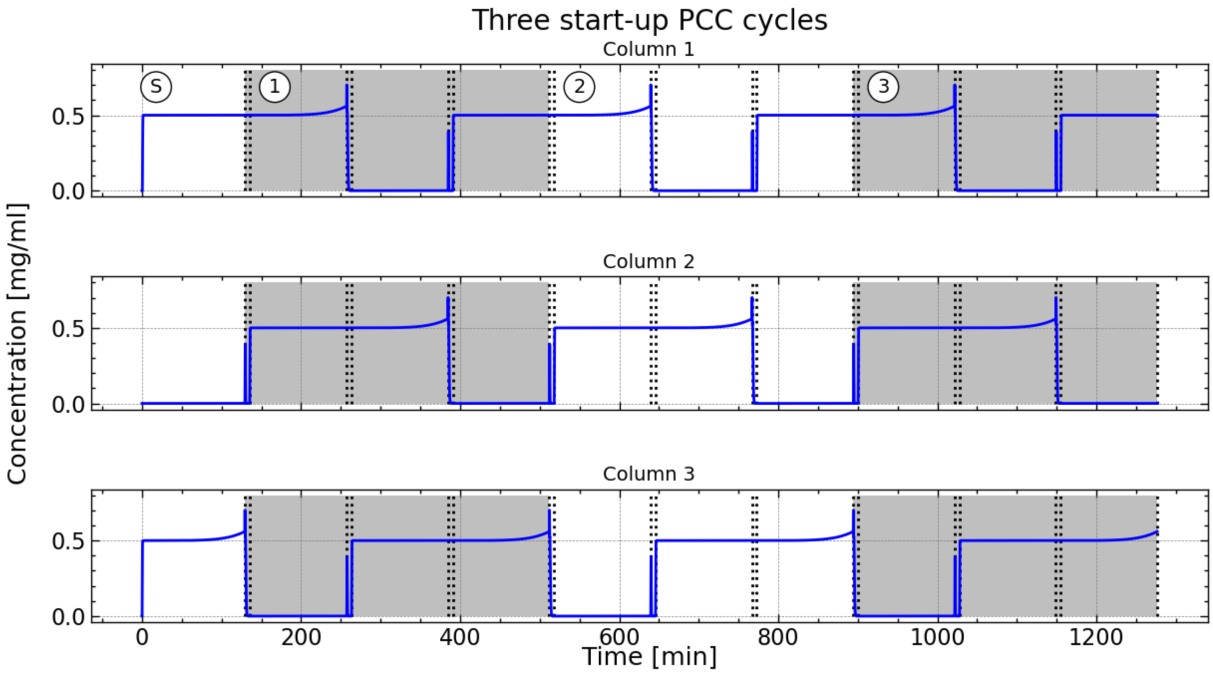

Figure 4.1 Three start-up PCC cycles. The three columns are loaded according to the PCC scheduling. Before the first cycle, column 3 and column 1 is coupled in series and loaded to start up the process. The white area for all columns beneath the "S"-symbol is the start-up phase. The first gray area from the left is the first cycle for all columns, marked with a circled 1. The second cycle is marked by the circled 2 and third cycles is marked by the circled 3. The dotted vertical lines indicate a phase shift.

Using the data in table 3.1, a degradation curve was found using a curve fit function. As seen in the figure 4.2, the data points appear random at first, but as the column degrades, and more data points are taken into consideration, a curve with good fit to the data appears. The value of a and b is -0.005 and 99.950 with a standard deviation of 0.0002 and 0.4806, of a and b respectively. The values of a and b fit the data well as the standard deviations are acceptably low.

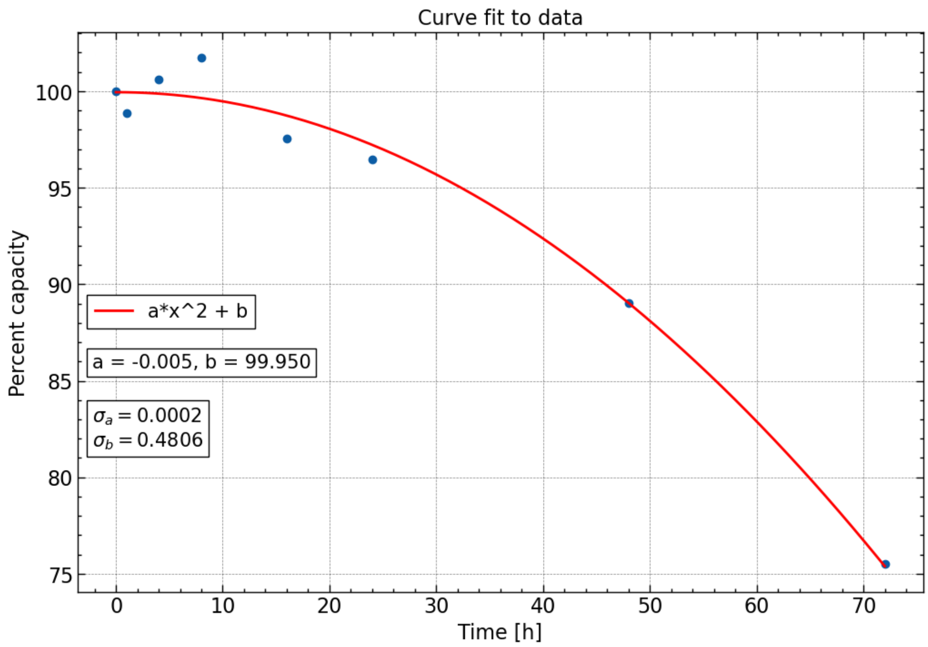

Figure 4.2. Curve fit to data from the degradation of active sites for the Äkta pure PrismA column. The data is fitted with a 2nd degree quadratic equation containing variables a and b.

In figure 4.2 the x-axis is the time the column has been in contact with sodium hydroxide, in hours. The columns are in contact with the sodium hydroxide for 15 minutes each cycle as part of the CIP procedure. The x-axis can be re-written in PCC cycles, assuming all columns start at 100% capacity and that they degrade according to the degradation curve. The points on the y-axis that are most interesting are 95%, 90%, 85%, 80%, and 75%. In table 4.1, the NaOH contact time, the cycle numbers and the column percent capacities that are used to present the results, are presented.

Table 4.1 Remaining column capacity percentage and the corresponding NaOH contact time and cycle number.

Percentage [%]	99.95	95	90	85	80	75
NaOH Contact Time [h]	2.25	26.25	37.25	45.75	53	58.75
Cycle number	9	105	149	183	212	235

The cases will be presented below in both figures and tables. In the tables, the process performance variables will be presented for the cycle numbers presented above in table 4.1.

4.1 Case 1 and 2

The results of case 1 and case 2 are presented in table 4.2.

Table 4.2 Process performance variables for Case 1 (A and B) and Case 2 (A and B).

CYCLE NUMBER	9	105	149	183	212	235
PERCENT CAPACITY	99.95	95	90	85	80	75
CASE 1A						
PRODUCTIVITY	0.180	0.180	0.180	0.180	0.180	0.180
YIELD	0.995	0.993	0.989	0.983	0.969	0.947
RESIN UTILIZATION	0.473	0.497	0.524	0.555	0.590	0.625
CASE 1B						
PRODUCTIVITY	0.163	0.163	0.163	0.163	0.163	0.163
YIELD	0.998	0.998	0.996	0.994	0.990	0.987
RESIN UTILIZATION	0.474	0.497	0.524	0.555	0.590	0.625
CASE 2A						
PRODUCTIVITY	0.172	0.172	0.172	0.172	0.172	0.172
YIELD	0.997	0.995	0.993	0.988	0.980	0.965
RESIN UTILIZATION	0.446	0.474	0.501	0.530	0.563	0.597
CASE 2B						
PRODUCTIVITY	0.157	0.157	0.157	0.157	0.157	0.157
YIELD	0.999	0.998	0.997	0.996	0.993	0.987
RESIN UTILIZATION	0.428	0.474	0.505	0.536	0.569	0.604

The flow trajectory has a noticeable effect on both systems with increased productivity, as seen in figure 4.3.1, but at the expense of yield at lower capacities and it does not affect the resin utilization in a significant way, see figure 4.2.3. Comparing case 1 and 2, the flow trajectory is influencing the yield, in that it’s decreasing at a faster rate, as seen in figure 4.3.2.

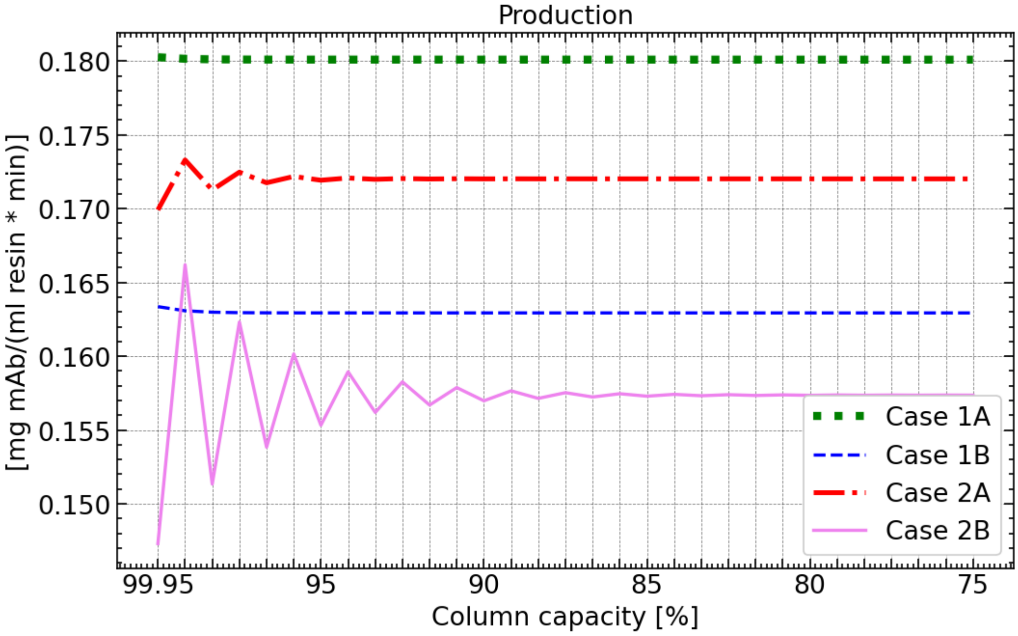

Figure 4.3.1 The production performance process variable as a function of the column capacity for Case 1 and Case 2. This figure is a visual representation of the data in Table 4.2.

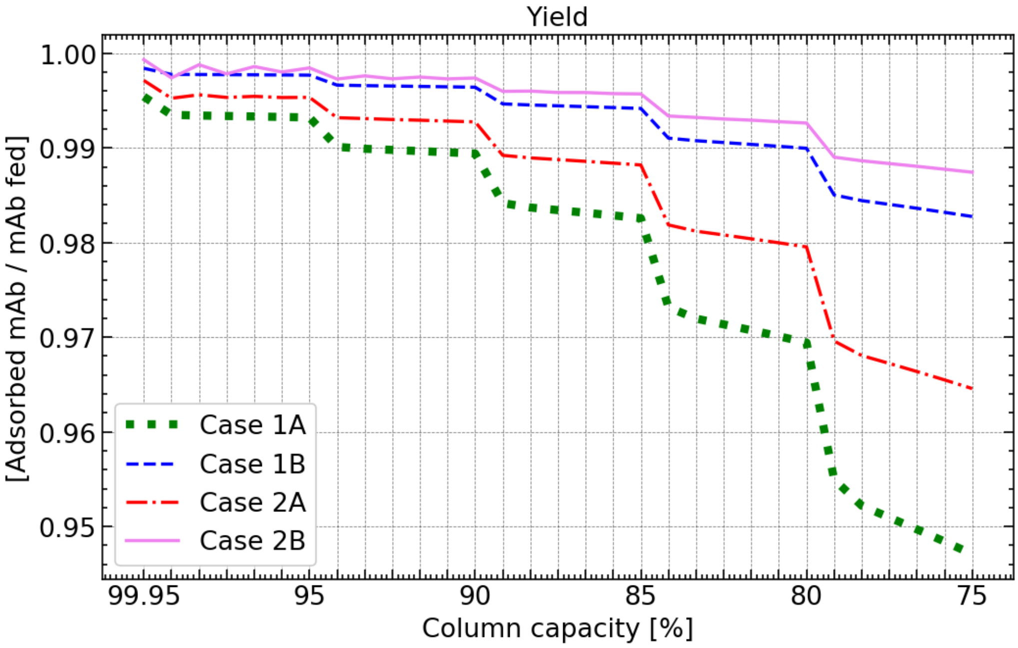

Figure 4.3.2. The yield performance process variable as a function of the column capacity for Case 1 and Case 2. This figure is a visual representation of the data in Table 4.2.

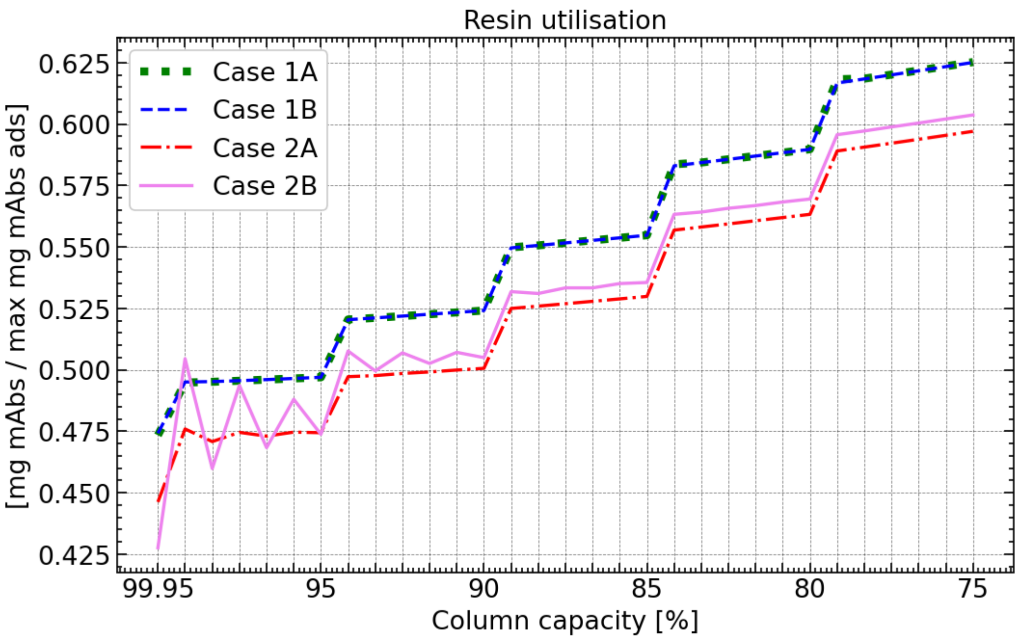

Figure 4.3.3. The resin utilization performance process variable as a function of the column capacity for Case 1 and Case 2. This figure is a visual representation of the data in Table 4.2.

4.2 Case 3 and 4

The simulation results for case 3 and 4 are presented in table 4.3.

Table 4.3 Process performance variables for Case 3 (A and B) and Case 4 (A and B).

CYCLE NUMBER	9	105	149	183	212	235
PERCENT CAPACITY	99.95	95	90	85	80	75
CASE 3A						
PRODUCTIVITY	0.116	0.116	0.116	0.116	0.116	0.116
YIELD	1.00	1.00	1.00	1.00	1.00	1.00
RESIN UTILIZATION	0.305	0.320	0.337	0.357	0.379	0.402
CASE 3B						
PRODUCTIVITY	0.105	0.105	0.105	0.105	0.105	0.105
YIELD	1.00	1.00	1.00	1.00	1.00	1.00
RESIN UTILIZATION	0.305	0.320	0.337	0.357	0.379	0.402
CASE 4A						
PRODUCTIVITY	0.202	0.202	0.202	0.202	0.202	0.202
YIELD	0.989	0.983	0.972	0.954	0.921	0.880
RESIN UTILIZATION	0.531	0.557	0.588	0.622	0.661	0.701
CASE 4B						
PRODUCTIVITY	0.202	0.202	0.202	0.202	0.202	0.202
YIELD	0.991	0.986	0.976	0.962	0.935	0.900
RESIN UTILIZATION	0.586	0.616	0.650	0.688	0.721	0.775

Case 3A and 3B has very high yields at the expense of productivity and resin utilization, as seen in the figures below. Case 3A has better productivity than 3B. Case 4A and 4B has a constant productivity and high resin utilization, at the expense of yield. This option would be viable if the product output was of greater importance than the losses. The yield loss tendency for cases with flow trajectory is visible when comparing 4A and 4B as well. The data in table 4.3 is visualized in figure 4.4.1, 4.4.2 and 4.4.3.

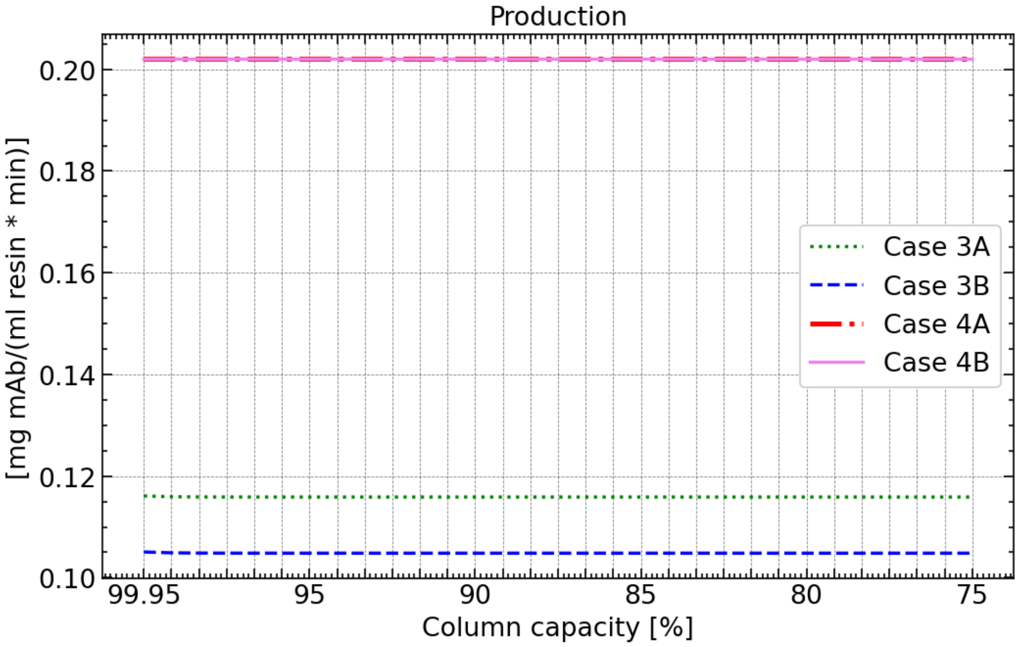

Figure 4.4.1. The production performance process variable as a function of the column capacity for Case 3 and Case 4. This figure is a visual representation of the data in Table 4.3.

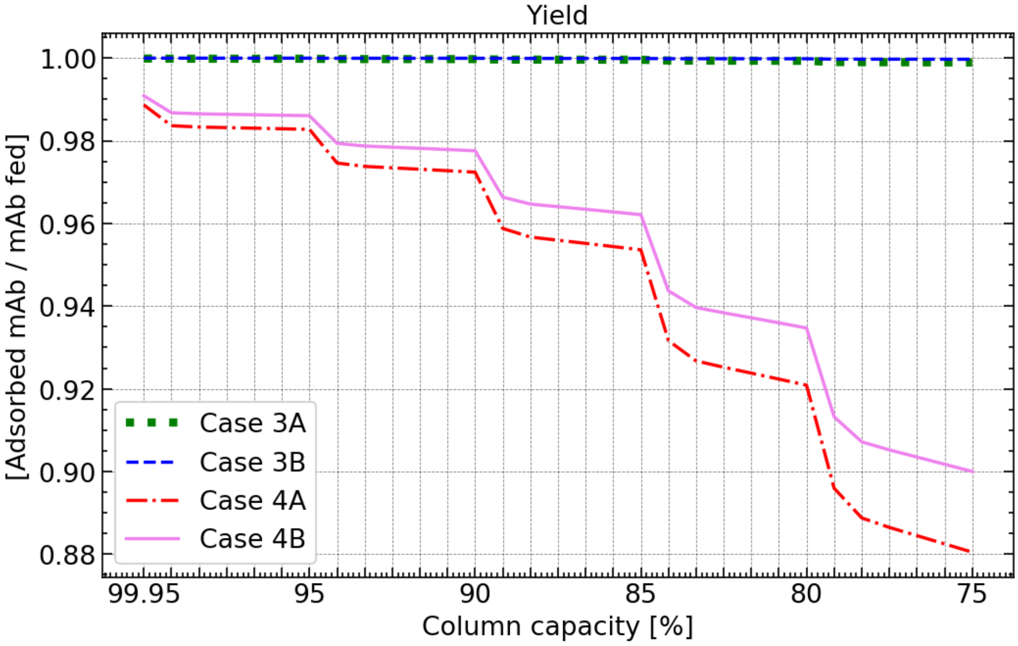

Figure 4.4.2. The yield performance process variable as a function of the column capacity for Case 3 and Case 4. This figure is a visual representation of the data in Table 4.3.

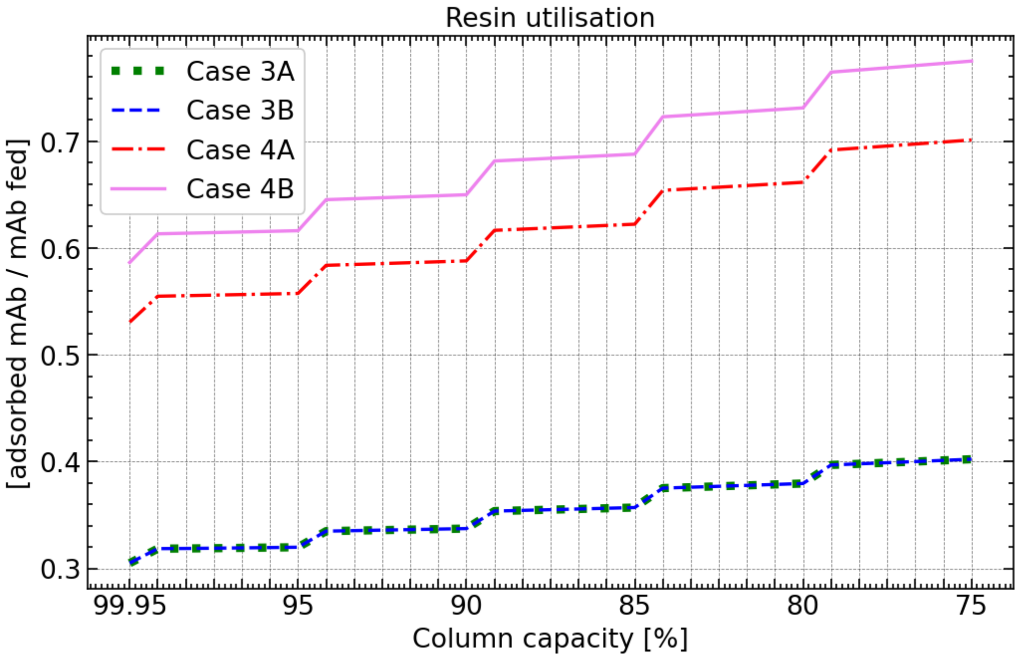

Figure 4.4.3. The resin utilization performance process variable as a function of the column capacity for Case 3 and Case 4. This figure is a visual representation of the data in Table 4.3.

4.3 Signal response for Case 1 through 4

The cases presented so far has had converging control signal outputs, as seen in figure 4.5. There are however some oscillations early in the simulation for Case 1B and 2B. With a moderately aggressive flowrate regulator (0.3) and a slow volume regulator (0.8), the two controllers counteract each other which is the cause for the oscillations.

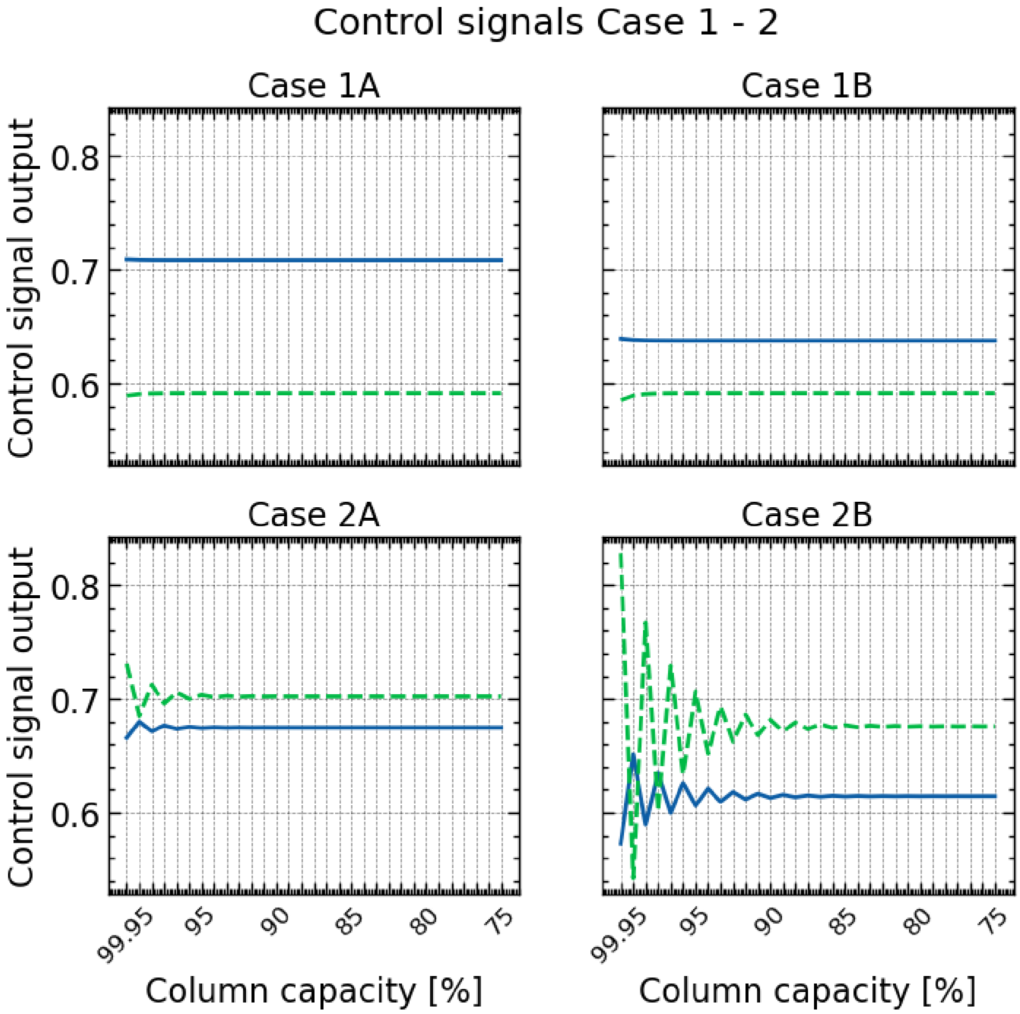

Figure 4.5. Control signal outputs for Case 1A through 2B, where the normalized flowrate signal is the blue line, and the volume regulation control signal is the green dashed line. Reference values are 1 for both signals in this figure.

For the Case 3, only the flowrate controller was activated with a parameter a of 0.3. Case 3A finds a steady signal slightly higher than Case 3B, due to the influence of the flow trajectory. For Case 4, only the volume regulation controller was activated with a parameter a of 0.3. The signal output was even from the start of the simulation, higher for Case 4A and lower for Case 4B, due to the flow trajectory, once again. The results can be seen in figure 4.6.

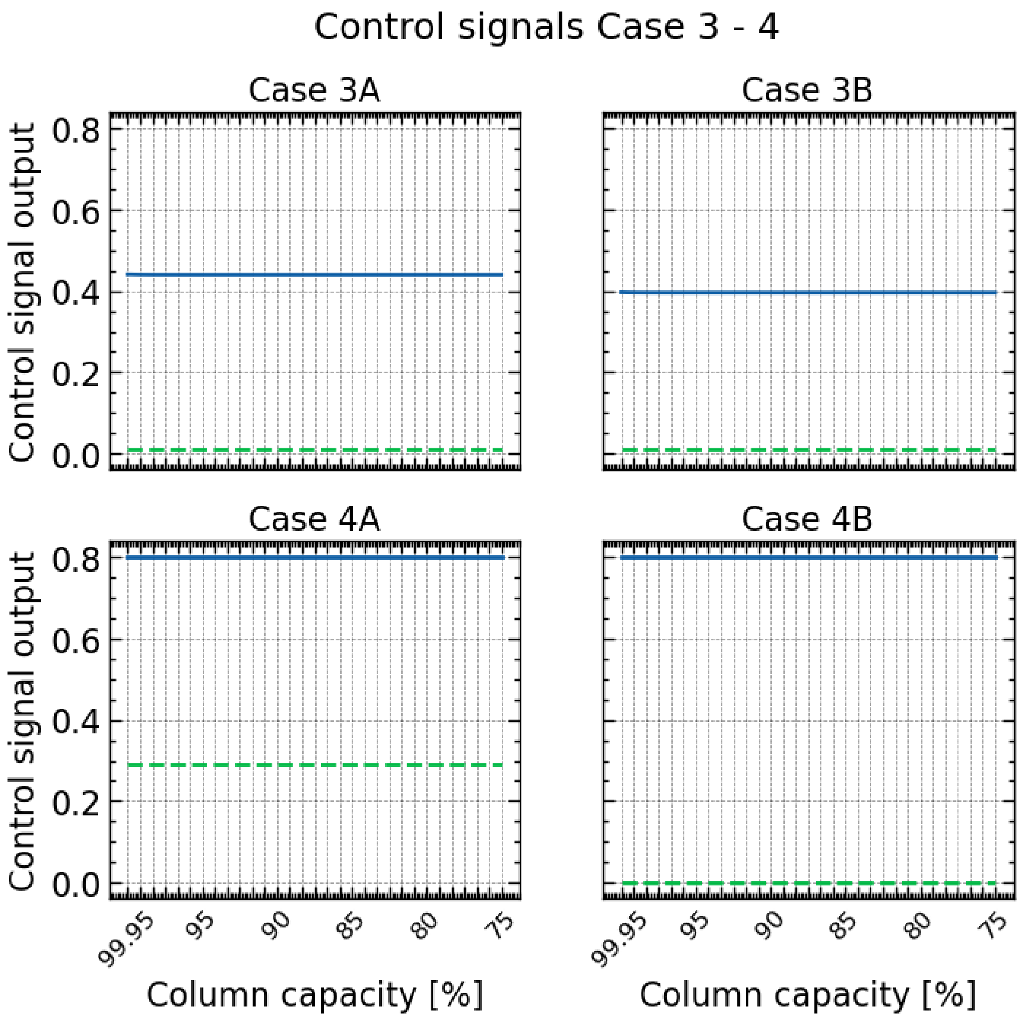

Figure 4.6. Control signal outputs for Case 3A through 4B, where the normalized flowrate signal is the blue line, and the volume regulation control signal is the green dashed line. Reference values are 1 for both signals in this figure.

4.4 Special cases X1 – X4

In the table 4.4. below, the four cases X1 through X4 are presented.

Table 4.4 Process performance variable results for Case X1, Case X2, Case X3, and Case X4.

CYCLE NUMBER	9	105	149	183	212	235
PERCENT CAPACITY	99.95	95	90	85	80	75
CASE X1						
PRODUCTIVITY	0.160	0.162	0.165	0.167	0.169	0.171
YIELD	0.998	0.997	0.995	0.990	0.981	0.964
RESIN UTILIZATION	0.419	0.448	0.480	0.515	0.554	0.593
CASE X2						
PRODUCTIVITY	0.156	0.152	0.145	0.124	0.082	0.082
YIELD	0.998	0.998	0.988	0.973	1.00	1.00
RESIN UTILIZATION	0.410	0.419	0.421	0.382	0.270	0.286
CASE X3						
PRODUCTIVITY	0.167	0.172	0.175	0.176	0.176	0.177
YIELD	0.997	0.995	0.992	0.986	0.974	0.955
RESIN UTILIZATION	0.439	0.475	0.509	0.542	0.578	0.613
CASE X4						
PRODUCTIVITY	0.163	0.165	0.167	0.168	0.169	0.171
YIELD	0.998	0.997	0.994	0.990	0.981	0.963
RESIN UTILIZATION	0.428	0.455	0.485	0.518	0.555	0.592

The table does not fully convey the behavior of the system as both divergence and oscillations occur for these cases. Case X2 reaches the lower simulation limit for the flowrate control parameter shortly after cycle 183 due to divergence. The two controllers were purposefully set with parameters that caused the controller inputs to oscillate with larger and larger amplitude. The results are not only visible for the control signals in figure 4.8, but also for the performance process variables in figure 4.7.1, 4.7.2, and 4.7.3.

Case X1 and X4 have very similar control signal responses and process performance, with slowly converging oscillations throughout the entire simulation. In Case X4, the flowrate control parameter spread for the columns can counteract the more aggressive volume regulation controller. Case X3 is the system in this grouping that converges within the cycle limit, with the highest productivity, but as seen before, the yield degrades faster for this case, than for Case X1 and X4.

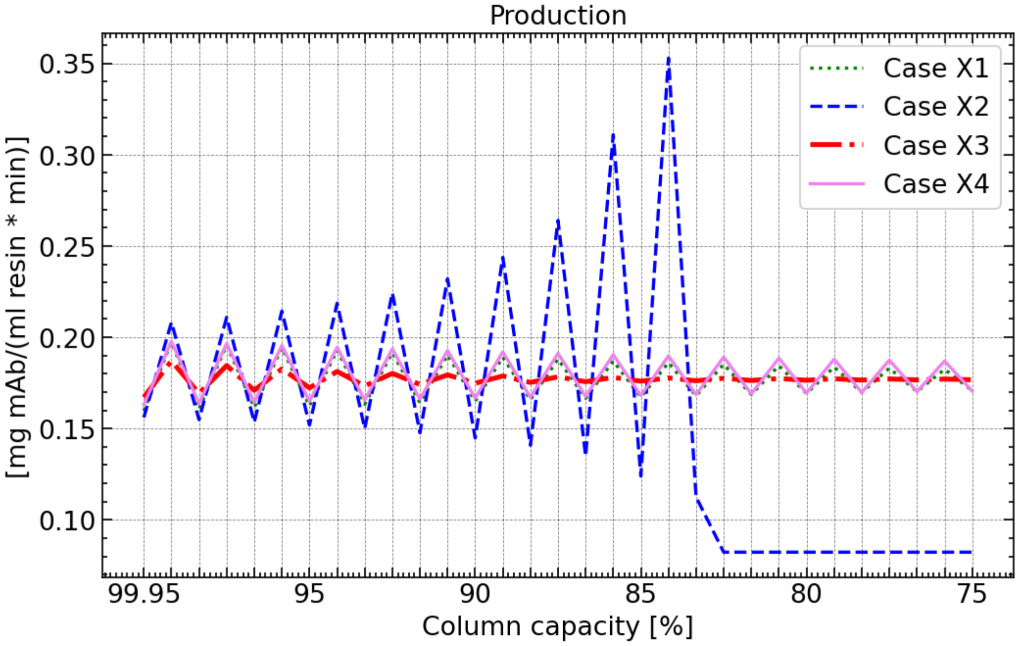

Figure 4.7.1. The production performance process variable as a function of the column capacity for Case X1 through Case X4. This figure is a visual representation of the data in Table 4.4.

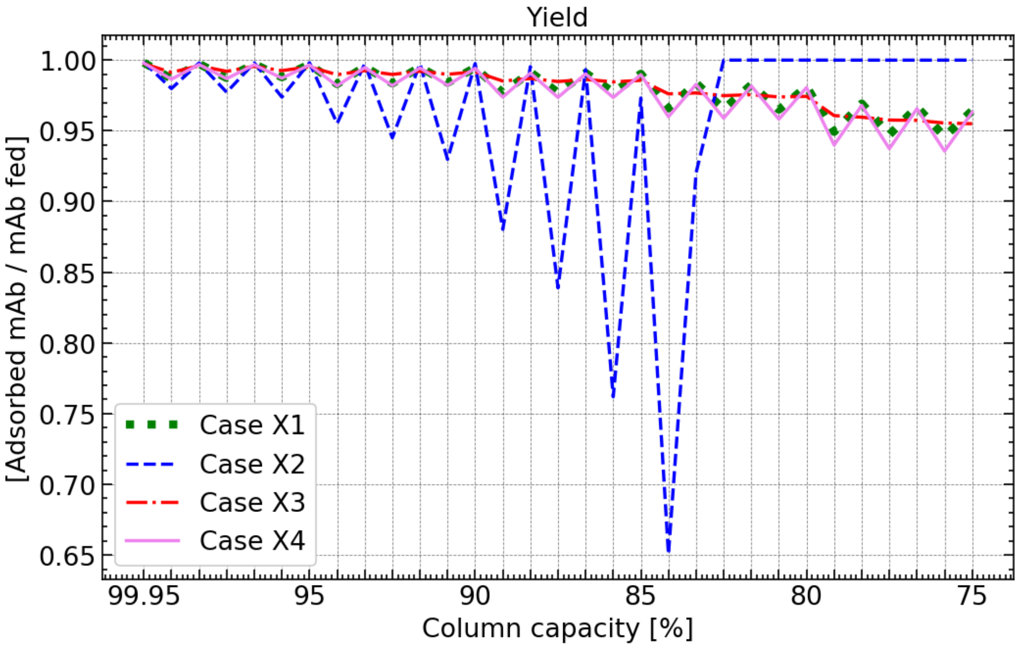

Figure 4.7.2. The yield process performance variable as a function of the column capacity for Case X1 through Case X4. This figure is a visual representation of the data in Table 4.4.

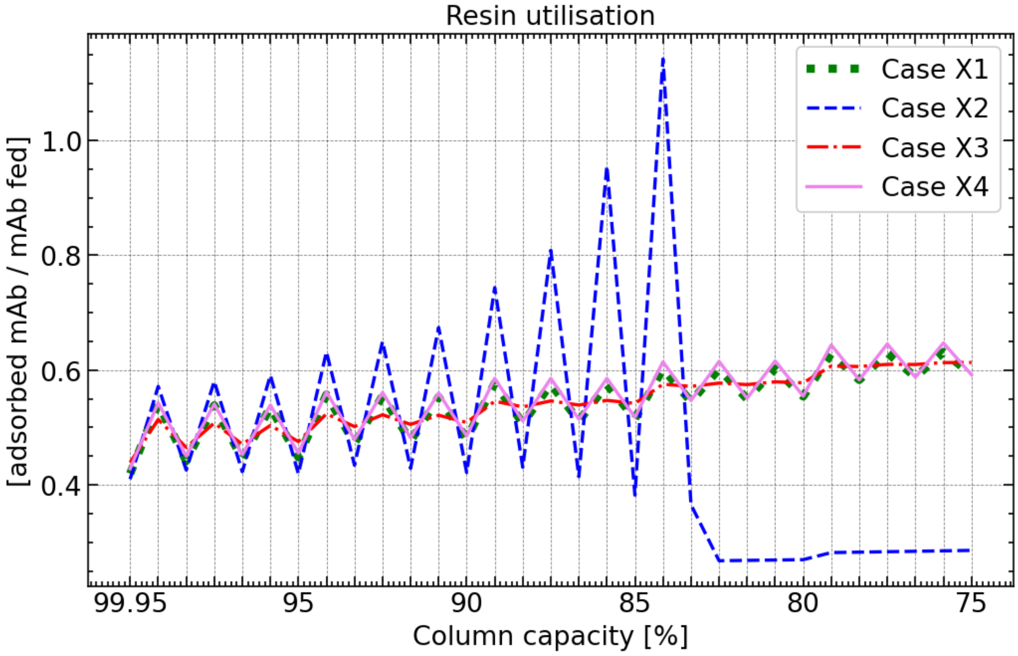

Figure 4.7.3. The resin utilization process performance variable as a function of the column capacity for Case X1 through Case X4. This figure is a visual representation of the data in Table 4.4.

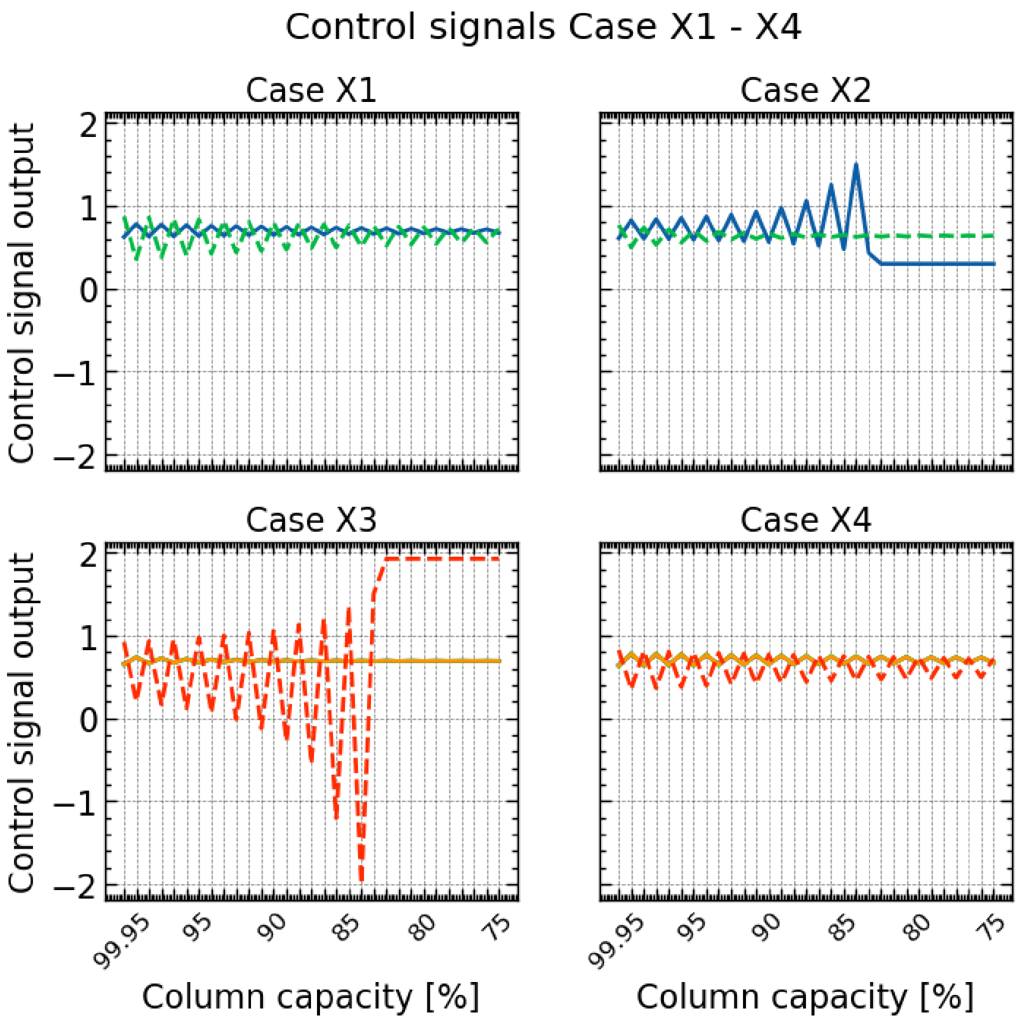

Figure 4.8. Control signals for Case X1 through X4, where the flowrate input signal is the blue line, and the volume regulation control signal is the green dashed line. Control signal outputs for Case X1 through X4, where the normalized flowrate signal is the blue line for case X1 and X2, and the orange line for X3 and X4, and the volume regulation control signal is the green dashed line for X1 and X2, and the red dashed line for X3 and X4. Reference values are 1 for both signals in this figure.

4.5 Discussion points

Case 4B is a good representation of what the process performance look like when no control is applied. The best alternative to counteract the tendencies seen in Case 4D is to apply the controller used in either Case 1A or 1B, to achieve high productivity, high yield. Case 1A and 1B had very smooth signal response curves as well.

The yield and resin utilization were affected by the column degradation because of a decision made early in the design of the simulation. The decision to keep the load time constant throughout the simulation. The productivity was not reduced by the resin degradation, this is because the starting cut-off percentage was only 6%. As the resin capacity decreased, so did the dynamic binding capacity, the cut-off percentage increased as mAb started eluting from the first column earlier and earlier. It never got to a point where the first columns capacity was completely utilized, but the resin utilization was heading in that direction.

The degradation curve was created under the assumption that 1M NaOH would be used for the CIP-phase. If the concentration was lower, the degradation would be slower and the lifetime of the column would be extended (ignoring fouling caused by HCP or other impurities in the feed solution), but the risk of contamination increases.

It would have been interesting to investigate controllers that kept yield and/or resin utilization constant if the time allowed for it.

5. Conclusions

The best case found was Case 1A, with a constant productivity at 0.18 mg mAb per ml resin and minute, a yield ending at 94.7% and a resin utilization ending at 62.5%. The controller settings were 0.8 for the flowrate parameter, and 0.3 for the volume regulation parameter. The flow trajectory was applied, which increased productivity at the price of a faster decline of the yield with lower resin capacities.

5.1 Future Work

- Investigating configurations with columns in different states of degradation.
- Varying the individual degradation of each column
- Optimizing the process from a bigger perspective to develop a dynamic controller that calculates when a column needs to be replaced to maintain certain process performance variables

6. References

Castelli, M. S., P. McGonigle and P. J. Hornby (2019). "The pharmacology and therapeutic applications of monoclonal antibodies." Pharmacol Res Perspect **7**(6): e00535.

Cytiva (2020). "Lifetime performance study of MabSelect™ PrismA during repeated cleaning-in-place cycles."

Danielsson, Å. (2018). Chapter 17 - Affinity Chromatography. Biopharmaceutical Processing. G. Jagschies, E. Lindskog, K. Łącki and P. Galliher, Elsevier**:** 367-378.

Diefenbach-Streiber, B., M. Enzelberger, J. Kölln, J. Prassler and M. Tesar (2010). "Monoclonal Antibodies." Ullmann's Encyclopedia of Industrial Chemistry.

Ebersbach, H. and S. Geisse (2012). "Antigen generation and display in therapeutic antibody drug discovery -- a neglected but critical player." Biotechnol J **7**(12): 1433-1443.

Gomis-Fons, J., N. Andersson and B. Nilsson (2020). "Optimization study on periodic counter-current chromatography integrated in a monoclonal antibody downstream process." Journal of Chromatography A **1621**: 461055.

Gomis-Fons, J., M. Yamanee-Nolin, N. Andersson and B. Nilsson (2021). "Optimal loading flow rate trajectory in monoclonal antibody capture chromatography." J Chromatogr A **1635**: 461760.

Hage, D. S. (2012). "Affinity Chromatography." Encyclopedia of Analytical Chemistry.

Hwang, Y. C., R. M. Lu, S. C. Su, P. Y. Chiang, S. H. Ko, F. Y. Ke, K. H. Liang, T. Y. Hsieh and H. C. Wu (2022). "Monoclonal antibodies for COVID-19 therapy and SARS-CoV-2 detection." J Biomed Sci **29**(1): 1.

Jagschies, G. (2018). Chapter 28 - Continuous Capture of mAbs—Points to Consider and Case Studies. Biopharmaceutical Processing. G. Jagschies, E. Lindskog, K. Łącki and P. Galliher, Elsevier**:** 527-556.

Lofgren, A., J. Gomis-Fons, N. Andersson, B. Nilsson, L. Berghard and C. Lagerquist Hagglund (2021). "An integrated continuous downstream process with real-time control: A case study with periodic countercurrent chromatography and continuous virus inactivation." Biotechnol Bioeng **118**(4): 1664-1676.

Longman, R. W. (2010). "Iterative learning control and repetitive control for engineering practice." International Journal of Control **73**(10): 930-954.

Lu, R. M., Y. C. Hwang, I. J. Liu, C. C. Lee, H. Z. Tsai, H. J. Li and H. C. Wu (2020). "Development of therapeutic antibodies for the treatment of diseases." J Biomed Sci **27**(1): 1.

Strube, J., S. Zobel-Roos and R. Ditz (2019). "Process-Scale Chromatography." Ullmann's Encyclopedia of Industrial Chemistry: 1-47.

Wetterhall, M., M. Ander, T. Bjorkman, S. Musunuri, R. Palmgren and G. Rodrigo (2021). "Investigation of alkaline effects on Protein A affinity ligands and resins using high resolution mass spectrometry." J Chromatogr B Analyt Technol Biomed Life Sci **1162**: 122473.

7. Appendices

Appendix A

Constants in the simulation, description, their values, and units			
D_{ax}	Axial dispersion coefficient	3.5e-1*v	cm^2/min
v	Superficial fluid velocity	[Changes]	cm/min
ε_c	Column void	0.34	-
r_p	Particle radius	3.00e-3	cm
L	Column length	2.5	cm
k_f	Particle mass transfer coefficient	4.9e-2*v^(0.58)	cm/min
F	Volumetric flow	[Changes]	ml/min
c	mAb solution concentration outside of particle	[Changes]	mg/ml
c_p	mAb solution concentration inside particle	[Changes]	mg/ml
D_{eff}	Effective pore diffusivity	3.89e-5	ml/mg
ε_p	Particle porosity	0.92	-
q1, q2	Adsorbed mAb onto particle	[Changes]	mg/ml
k_1, k_2	Adsorption rate constants	2.65, 2.34e-2	ml/(mg*min)
$q_{max,1}$, $q_{max,2}$	Maximum adsorption capacity	43.56, 100.83	mg/ml
K	Langmuir equilibrium constant	20.9	ml/mg
V_c	Column volume	1.0	ml